Data-Driven Modeling of 4D Ocean and Coastal Acidification from Surface Measurements

B. Champenois[1], C. Bastidas[2], B. LaBash[3], T. P. Sapsis[1]

[1]Massachusetts Institute of Technology, Cambridge, MA 02139
[2]Massachusetts Institute of Technology, Sea Grant College Program, Cambridge, MA 02139
[3]Northeastern University, Boston, MA 02115

Key Points:

- We present a data-driven approach to rapidly model 4D carbonate chemistry fields given readily available surface observations.
- By using training data from both physics simulations and field observations, the model achieves very high resolution with minimal inputs.
- The step-by-step method can be reproduced in other regions or for new data, and includes uncertainty quantification for decision making.

Corresponding author: Bianca Champenois, `bchamp@mit.ed`

Abstract

A significant portion of atmospheric CO_2 emissions is absorbed by the ocean, resulting in acidified seawater and altered carbonate composition that is harmful to marine life. Despite detrimental effects, understanding the severity of ocean and coastal acidification (OCA) is difficult due to the scarcity of in-situ measurements and the high costs of computational modeling. We develop a parsimonious data-driven framework to model indicators of OCA, and we test the framework in the Massachusetts Bay and Stellwagen Bank, a region with considerable fishing and tourism industries affected by OCA. First, we trained a neural network to predict in-depth fields for temperature and salinity (x, y, z) using surface quantities from satellites and in-situ measurements (x, y). The relationship between 2D surface and 3D properties is captured through the in-depth modes and coefficients obtained from principal component analysis applied to a high-resolution historical reanalysis data set. Next, we used Bayesian regression methods to estimate region-specific relationships for in-depth total alkalinity (TA), dissolved inorganic carbon (DIC), and aragonite saturation state (Ω_{Ar}) as a function of in-depth temperature, in-depth salinity, and surface chlorophyll-a concentration. Lastly, 4D field predictions are made from surface measurements using the neural network followed by the regression models. The model's performance is evaluated using withheld measurements at multiple depths, locations, and seasons, and the near real-time predictions for temperature, salinity, TA, DIC, and Ω_{Ar} are useful for understanding the impacts and evolution of OCA. Each step of the framework includes uncertainty quantification which can be used for future planning and optimal sensor placement.

Plain Language Summary

About a quarter of carbon dioxide emissions in the atmosphere is absorbed by the oceans. When this carbon dioxide dissolves in seawater, it results in ocean acidification. A useful indicator of ocean acidification is the saturation state of aragonite, a type of calcium carbonate used by organisms that form shells. However, understanding the effects of ocean acidification is difficult due to the lack of observations and the high cost and complexity of modeling. We present a data-driven approach to model carbonate chemistry using readily available observations from satellites and low-cost sensors. Given surface measurements of temperature, salinity, and chlorophyll, our machine learning model produces temperature, salinity, total alkalinity, dissolved inorganic carbon, and aragonite saturation state covering spatial (latitude, longitude, depth) and temporal domains for these variables. Compared to withheld observations, our model achieved reasonable accuracy across many seasons and depths, a level of resolution not matched by other models for the same set of inputs. Our model is useful for monitoring, decision making, and future planning.

1 Introduction

1.1 Ocean and Coastal Acidification

Each year, the oceans absorb approximately 9 billion tons of CO_2, corresponding to a quarter of atmospheric CO_2 emissions [1, 2]. Since the industrial revolution, these changes in the seawater-carbonate system have resulted in an approximately 30% increase in ocean acidity, a process called Ocean Acidification (OA), with a projected doubling of this increase by the end of the century [3, 4]. OA results in increased concentrations of dissolved inorganic carbon (DIC), increased partial pressure of carbon dioxide (pCO_2), and a lower pH. These changes in seawater decrease the availability of carbonate ions, affecting the state of saturation of calcium carbonate. The saturation state of aragonite (Ω_{Ar}), a type of calcium carbonate that many marine organisms use to build their shells [5] is a very important indicator of OA.

While OA is largely driven by atmospheric CO_2, other physical and biogeochemical processes (e.g. stratification, excess nutrients, and freshwater) can exacerbate acidification. The complex interplay of these processes in nearshore areas, referred to as Ocean and

Coastal Acidification (OCA), varies widely across seasons and regions. For example, OCA is particularly intensified along the coast of the US Northeast where heavy precipitation coupled with significant freshwater and nutrients from runoff lower the Total Alkalinity (TA) and lead to a reduced buffering capacity, especially in regions near estuaries [6]. In such conditions, pH and Ω_{Ar} can change more easily and more rapidly than in waters with high buffering capacity.

We focus specifically on the Massachusetts Bay (Mass Bay) and Stellwagen Bank, a nearshore subset of the larger Gulf of Maine (GOM) [7]. The impact of OCA in marine resources of the region has been extensively documented [8, 9], and recently reviewed [10]. Furthermore, this region has shown changes in physical characteristics such as increases in temperature and salinity, together with changes in summer wind patterns, which have been related to low bottom dissolved oxygen conditions when compared to the 1992-2000 baseline data [11, 12]. These types of changes are known to produce concurrent fluctuations of pH in nearshore ecosystems, are likely to exacerbate the impacts of OCA, and will particularly affect bottom dwellers such as lobsters, sand lance, and sea scallops that are key in the regional blue economy [13, 14, 15]. Monitoring and predicting OCA is crucial because coastal ecosystems such as those in the GOM sustain major fishery and tourism industries [16]. Beyond being harmful to commercially relevant fish and shellfish, OCA will have effects on a myriad of other marine species with mostly unknown ecological consequences, such as possible food web failures [17, 18].

Despite the negative biological and economic consequences of OCA, predictive capability is still limited, and efforts are being made to advance observation and the development of data products [19]. High-fidelity physics-based numerical models are unattainable for the foreseeable future due to the difficulty of modeling the multi-scale and multi-physics problem, which consists of complex physicochemical and biological processes, and their interactions with ocean currents and circulations. As an alternative, changes in OCA can be monitored with in-situ measurements, but the process of acquiring water samples over large domains at a high spatiotemporal resolution is expensive. Remote sensing is also a useful option, but measurements are often only available for certain quantities, they are at the surface, and they are often inconsistent (e.g. due to clouds). Empirical relationships are a promising hybrid approach, but in many cases, these types of models only provide estimates for indicators of OCA in locations where in-situ samples of explanatory variables are collected rather than for a full field. We propose a new data-driven framework which relies on a combination of data from all of the aforementioned sources. In our framework, we train a physics-informed machine learning (ML) model on data from a high-resolution numerical simulation, and we use this model to make predictions given in-situ measurements and satellite remote sensing data. Before going into the details of our own model, we discuss more examples and advancements of data-driven empirical models in the following section [20, 21, 22, 23, 24, 25, 26].

1.2 Empirical Models

The basis for our model was inspired by other models in the literature that use some form of regression to develop empirical relationships for the seawater-carbonate system between available quantities and quantities of interest.

One of the earlier papers on the development of empirical relationships for OA focused on the Pacific Northwest [20]. This study used a standard multiple linear regression model to predict Ω_{Ar} as a function of temperature, oxygen, and a temperature-oxygen interaction term with measurements between 30m and 300m during May 2007. The training root mean squared error (RMSE) for Ω_{Ar} was found to be 0.053, but no validation RMSE was reported, so it is difficult to assess the potential risk of model overfitting. A 2011 follow up study by Juranek et al. applied the same methodology to the Northeast Subarctic Pacific [21]. This study focused on measurements between 30m and 500m. Calibration (training) data was

collected between March 2006 and September 2008, and between February 2010 to early 2011. Validation data for one buoy (station P20) was collected between February and June 2010. The training RMSE was 4.8 μmol·kg^{-1} for TA, 3.5 μmol·kg^{-1} for DIC, and 0.052 for Ω_{Ar}. Again, no validation RMSE was reported.

Following these papers, Davis et al. 2018 published a similar study which focused on the Central California Current System (CCS) in Northern California [22]. The model was produced using training data that were collected up to three times annually (2012 - 2015) between May and September, and between depths of 27m and 227m. The validation data were collected yearly from five on-shelf locations along the Bodega Line, between 1m and 200m. Ω_{Ar} was modeled using multiple linear regression with temperature, salinity, dissolved oxygen, and interaction terms as regressors. The training and validation R^2 were found to be 0.92 and 0.79 respectively. No good relationship was found for data in September, so measurements from that month were excluded from training and validation.

In 2020, McGarry et al. published a new multiple regression model for the GOM [24]. The training data were collected in summer months between July and August 2007, July and August 2012, and June and July 2015. The validation data came from May 2013 to July 2015 and from June to July 2018. The validation RMSE in the GOM was 10.9 μmol·kg^{-1} for TA, 11.2 μmol·kg^{-1} for DIC, 0.038 for pH, and 0.148 for Ω_{Ar}. A 2020 paper by Lima et. al opted to use a neural network to model the empirical relationships between quantities of interest [25]. Like in the McGarry paper, this study also focused on the Gulf of Maine but used inputs from a few more sources of data including CTD data (temperature, salinity, depth), in-situ measurements of dissolved oxygen, satellite data (chlorophyll, turbidity, sea surface height, sea surface temperature), and atmospheric xCO_2. The model architecture consisted of 2 hidden layers, each with 256 neurons, LeakyRELU activation, batch normalization, and a learning rate of 0.01. 100 models were trained to predict DIC and TA, and the median standard deviation of the outputs was used as a metric for uncertainty. pH and Ω_{Ar} were then obtained with CO2SYS from TA and DIC. The best model achieved a test RMSE of 9.0 μmol·kg^{-1} for TA and 15.4 μmol·kg^{-1} for DIC. However, the models performed worse when dissolved oxygen measurements and/or satellite data were removed.

In addition to studies on the modeling of empirical relationships, there also exist studies on nutrients and carbonate chemistry which we used to inform choices regarding relationships between different variables. Rheuban et al. 2019 studied ocean acidification in Buzzards Bay in the Northeast [23], a region that is nearby to the region in our study. The average depth of the region of study was 11m, and measurements were used from June 2015 to September 2017 (year round). They collected measurements of temperature, salinity, TA, and DIC, and they used those to predict Ω_{Ar} using CO2SYS. They do not report any error metrics as there are no data to use as a benchmark, but they quantify the uncertainty with bootstrapping.

1.3 Framework Overview and Contributions

We draw from all of these past studies to produce our own framework. In this paper, we develop a regional OCA model that leverages machine learning to quickly and inexpensively predict 4D (x, y, z, t) indicators of OCA from just surface measurements of temperature (T), salinity (S), and chlorophyll-a concentration (Chl). An overview of the framework is outlined in Figure 1. First, in Section 3, we interpolate surface measurements of temperature, salinity, and chlorophyll-a concentration. These surface measurements (x, y) are obtained from satellites and CTD sensors. Next, in Section 4, we train a neural network (NN) to predict in-depth temperature and salinity from surface temperature and salinity. We train the NN model on a high-resolution historical reanalysis data set obtained from a physics-based numerical simulation. As a result, our model inherits knowledge of the physics of the system. In Section 5, we use standard regression techniques to develop an empirical model that maps temperature, salinity, and surface chlorophyll-a concentration to TA and DIC. Finally, in Section 6, we use an existing model of the seawater carbonate system to estimate Ω_{Ar}

from TA and DIC. In the end, we obtain 4D (x, y, z, t) predictions for temperature, salinity, TA, DIC, and Ω_{Ar}, and these predictions are made from in-situ and remote sensing surface measurements of temperature, salinity, and chlorophyll-a concentration. The framework is implemented as a server that makes and serves predictions on new data as it becomes available, with results visualized on an online platform. Server code and visualization are available at https://github.com/becklabs/aragonite-opendap.

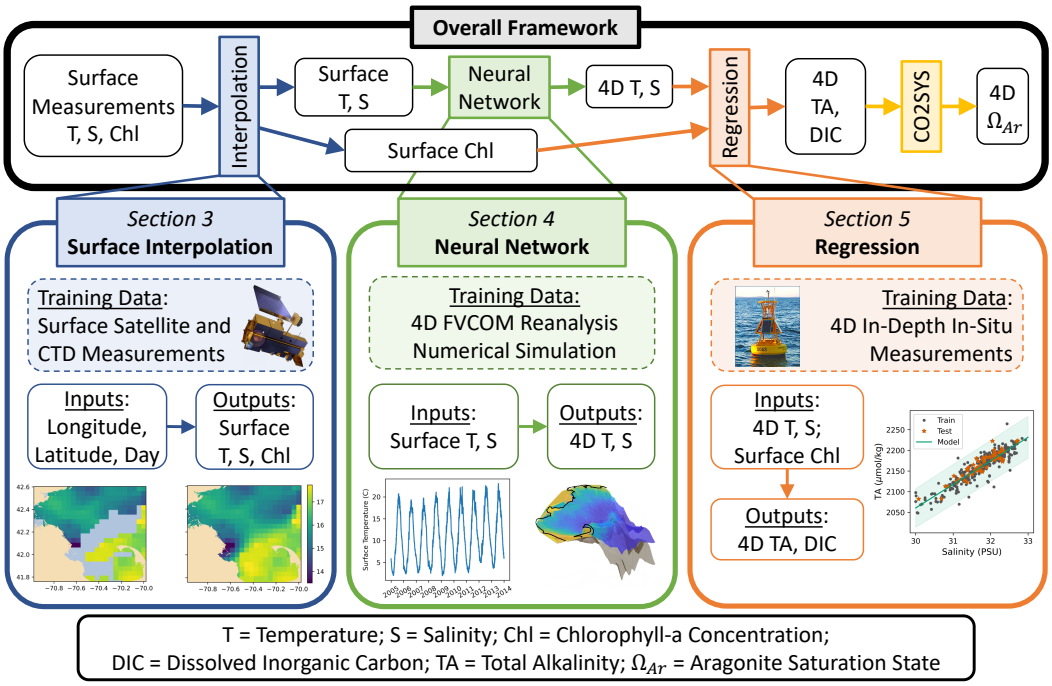

Figure 1: **Overview of framework**. In Section 3, available temperature, salinity, and chlorophyll-a concentration surface measurements are interpolated to obtain a 2D surface field. In Section 4, a neural network is trained on reanalysis data to predict 3D temperature and salinity from 2D temperature and salinity. In Section 5, standard Bayesian regression models are trained using in-situ observations to predict 3D TA and DIC from temperature, salinity, and surface chlorophyll. Finally, in Section 6, Ω_{Ar} is obtained from TA and DIC using the CO2SYS software.

Some key differences between our study and these existing studies are that we focus on a part of the ocean that is much closer to the coast for our region of interest, and we develop a model for a much wider range of years (2017-2023) and for all seasons. Furthermore, the whole framework is able to make in-depth predictions for DIC, TA, and Ω_{Ar} given only surface measurements of temperature, salinity, and chlorophyll-a concentration as opposed to other models which use in-depth in-situ measurements which are more expensive to collect. Because we use surface measurements, we are able to make predictions at a high resolution for a much larger spatial domain rather than just for locations at which in-situ samples are collected. In contrast to some of the existing models, our model is based on a physics-based numerical model which is why it is able to cover a larger domain of interest while remaining very fast. Like other empirical models, the nature of our model also makes it easily adaptable when new sensor data become available. Additionally, we use regression and machine learning methods that are more suitable for modeling nonlinear relationships, and we also use Bayesian methods to estimate uncertainty.

We demonstrate the success of our method at one location seen during model training (station F22) and one location not seen during model training (station F06) for a wide range of depths and years, but the framework can be extended to model the entire region at a high resolution. The method can also be replicated in other regions for which a comprehensive numerical ocean model exists.

2 Data

The strength of our model comes from the fact that we are combining a variety of different sources of data. We use high-resolution 4D data obtained from a numerical simulation to train a neural network that can predict in-depth temperature and salinity from surface measurements. To obtain these surface measurements, we use low-cost and widely available satellite data to cover a larger domain of interest. We use a few hundred high-fidelity in-situ samples to develop empirical relationships between variables that are easy to measure and sought-after quantities that are more expensive to collect. The different data sources are summarized in Table 1.

Table 1: Data sources and variables used in the framework.

Variable	FVCOM	Satellite	In-Situ Measurements (3D)
Temperature	3D field	2D surface field	4413 points
Salinity	3D field	N/A	4406 points
Chlorophyll-a	N/A	2D surface field	N/A
TA	N/A	N/A	538 points
DIC	N/A	N/A	538 points
Ω_{Ar}	N/A	N/A	538 points (estimated from TA and DIC)

2.1 Numerical Simulation: Temperature and Salinity

We use a high-resolution, high-fidelity, physics-informed data set to train a machine learning model that can predict temperature and salinity in depth from temperature and salinity at the surface. The data set we use comes from the Finite Volume Community Ocean Model (FVCOM), a historical reanalysis data set of temperature and salinity in the Massachusetts and Cape Code Bays from 2005 to 2013 [27]. More details about the numerical simulation can also be found in Champenois and Sapsis [28].

2.2 Satellite: Temperature and Chlorophyll

We obtain daily sea surface temperature and surface chlorophyll from Level 3 Aqua-MODIS between 2017 and 2023 [29]. The Aqua-MODIS satellite has been measuring visible and infrared radiation for the whole Earth every one to two days since 2002. To simplify the framework, we only use data from Aqua-MODIS, and we only use daytime measurements (as opposed to nighttime) but future work could be done to incorporate data from other satellite products such as Terra-MODIS or Sentinel-3 OLCI. The satellite data have been processed to translate radiation into temperature and chlorophyll-a concentration. The obtained data set is referred to as Level 3 because it it has not yet been interpolated to account for gaps due to cloud coverage. We perform this interpolation in Section 3.

2.3 In-Situ Observations: Temperature, Salinity, TA, DIC

In addition to the numerical model and satellite measurements, we have access to monthly in-situ measurements of physical and biological conditions, and to less frequent laboratory determinations of DIC and TA, at multiple depths and sites. These in-situ measurements and the collection of water samples for DIC and TA determinations were made by the Massachusetts Water Resources Authority (MWRA) and other local organizations [11] and by MIT Sea Grant. These data were obtained between February 2017 and November 2022, with no observations made for the months of December and January during that period.

In-situ measurements of the water column were taken nine times per year at eleven stations in Mass Bay and three stations in Cape Cod Bay and Stellwagen National Marine Sanctuary (SBNMS) (Libby et al. 2024). At each sampling time, all stations are sampled in a day with a CTD system, an inexpensive device that measures conductivity, temperature, and depth, and various other sensors (DO, pH, light irradiance, among others). Water samples for DIC and TA were collected at F22, F23, N04 and N18 in 2017, and at F22, F06, N01 and N07 between 2018 and 2022 (see Figure 2). At these stations, water samples were collected using a Rosette equipped with up to twelve 9L Niskin bottles. At each station, water samples were collected during the upcast at three depths (1-2m, mid-, and deep-water), with duplicates collected at mid-depths in two of the stations. The depth of mid- and deep-water samples vary among stations, with the deepest ones taken at 79m in F22. Other sites were sampled opportunistically within the geographic area and time frame of this study (2017-2022) using a 5L Niskin bottle for the water collection at each depth. These other sites include: a) thirty-one stations sampled at the SBMNS within two days in July of 2018 (n=45 samples: 34 of them collected at 1-2m and 11 collected at 25-26m deep); and, b) nine stations within the Boston Harbor, which were sampled in 2017, 2018 and 2019 at a maximum depth of 18m (n=98 samples). All water samples were collected in borosilicate bottles of 300 mL following best practices [30]. After collection, samples were preserved with 130 μL of a saturated mercuric chloride solution and were sealed with stoppers using Apiezon M grease. Samples were refrigerated until analysis in the lab. Samples were analyzed for DIC via coulometry and TA via closed-cell potentiometric Gran Titration with a VINDTA 3C (Marianda Corporation). For 2022 samples, the TA was measured by open cell HCl titration using a custom system designed and built by the laboratory of Andrew Dickson (University of California, San Diego). The instrument is the same type used to certify CRMs for TA [31].

The in-situ data were obtained from the MWRA Environmental Quality Department (ENQUAL). These data were collected from a variety of sources, for a variety of different uses and with different standards for accuracy and precision. Data accepted into the ENQUAL database are subjected to further in-house quality assurance procedures which are continually being refined. As the data were updated or qualified as new errors were found, we contacted ENQUAL to ensure that we were using the latest set of data. Measurements made by in-situ sensors and determinations made in the lab from water samples were stored in separate data sets. To synchronize these data sets we joined them spatiotemporally, on a per day basis, using 1e-6, 1e-6, and 3m as matching thresholds for latitude, longitude, and depth respectively. With these parameters, no ambiguities were detected in the matches.

3 Extrapolating Temperature, Salinity, and Chlorophyll Surface Data

To account for the lack of complete spatial and temporal coverage of the satellite data and in-situ surface measurements, we use Gaussian process regression to estimate full 2D surface fields [32, 33, 28]. In the case of temperature, the surface measurements can come either from satellites or in-situ samples. For chlorophyll-a concentration, we exclusively use the satellite data. For salinity, only in-situ measurements are available for the scale and region of interest, and they are commonly collected with a CTD.

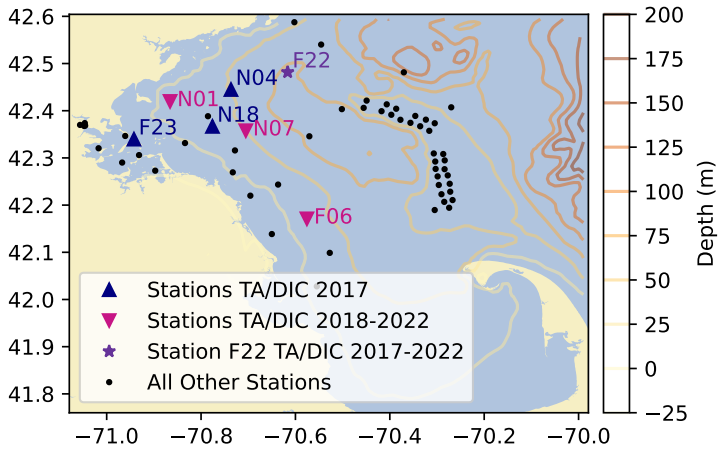

Figure 2: Location of stations for in-situ observations in the region of the study, encompassing Massachusetts Bay and Stellwagen Bank within the Gulf of Maine.

For satellite data, we use the interpolation method described in Champenois and Sapsis to interpolate between gaps caused by cloud coverage [28]. In this method, Gaussian process regression is repeatedly performed for each day using data from the previous, current, and following day. By only using three days of data at a time, there is no limitation caused by the need to invert large matrices. For chlorophyll-a concentration, we use a log transformation to reduce skewness, address different scales of variability, and improve uncertainty predictions. An example of the extrapolation for temperature is shown in Figure 3.

For in-situ data, we use Gaussian process regression using all of the available training data to interpolate between days and locations at which samples are taken. Like with the satellite data, we use a standard squared exponential covariance function (also known as the radial basis function). Instead of optimizing the marginal likelihood, we manually set the hyperparameters of the covariance function (lengthscale, signal variance, and noise variance) to overcome problems caused by highly infrequent sampling.

4 Deriving In-Depth Temperature and Salinity Fields from Surface Measurements

We build on the framework from Champenois and Sapsis to predict both temperature and salinity in three dimensions from surface sensor measurements using a neural network applied to data from a physics-based model [28]. Temperature and salinity are conservative variables, so they are governed by transport laws (passive scalar advection-diffusion) and are therefore more suitable for physics-based modeling. We modify the framework by applying it to the anomaly data instead of the original data. The anomaly is obtained by subtracting the climatology from the original data field, and the climatology is the annual mean over the nine years of data. The model is trained on seven years of the FVCOM using the same neural network architecture and hyperparameters from Champenois and Sapsis [28].

4.1 Model Order Reduction with Principal Component Analysis

First, we compute the climatology and anomaly of the FVCOM data set. Then, we apply principal component analysis (PCA) to the FVCOM anomaly data [34, 28]. This allows us to represent the vertical structure of temperature and salinity as a function of just a temporal mean and two modes with corresponding time coefficients. Results from the

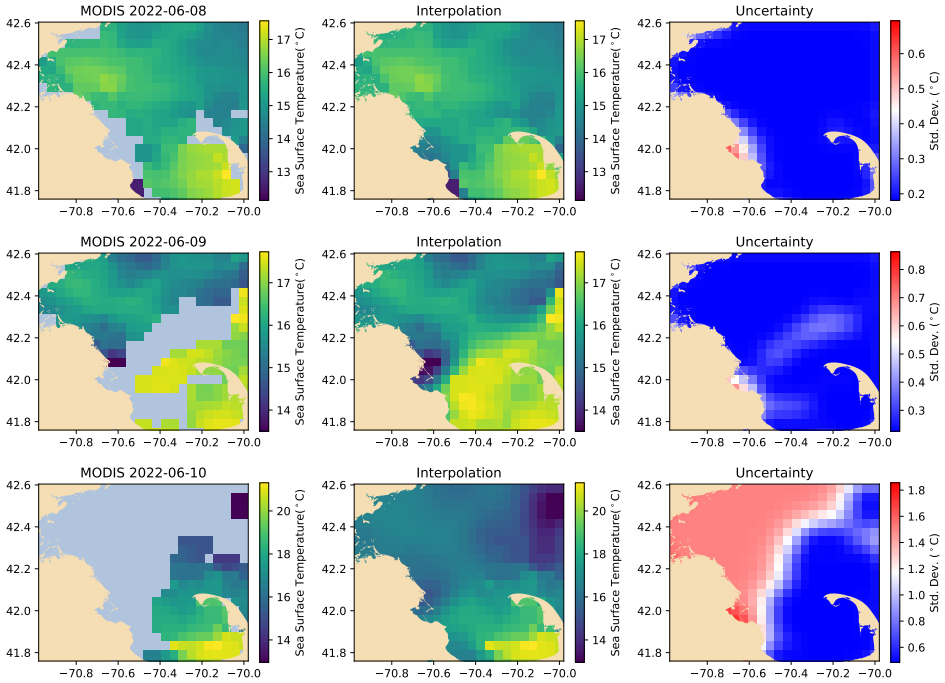

Figure 3: **Sea Surface Temperature Interpolation from Satellite Data**. The left columns shows unprocessed MODIS data, the center column shows the interpolation obtained with Gaussian process regression, and the right columns shows the uncertainty associated with the prediction. Each row shows a different day between June 8-10, 2022.

PCA are shown in Figure 4 where we show the modes, the coefficients, and the percentage of variance capture by each mode. The first vertical mode captures inputs from the surface, and the second mode captures smaller-scale effects brought about by the mixing layer. We only use two modes as these capture more than 95% of the variance.

4.2 Neural Network Predictions from Surface Measurements

Next, we train a temporal convolutional neural network (TCN) to predict the time-varying coefficients of the PCA modes as a function of surface properties [35, 28]. A TCN is a neural network architecture that uses causal convolutions to make predictions from time series. We use surface properties as the predictors because they are readily available from real-world sensors. As in [35] and [28], we also train a second TCN to predict the standard deviation of the variables. The process is very similar to the one described in [28] with the exception that we use anomaly data (de-trended) for training.

Finally, we input the real-time 2D surface estimates into the neural network to obtain probabilistic predictions for the coefficients of the PCA modes, and we obtain the full 3D prediction by combining the newly predicted PCA coefficients with the PCA modes.

4.3 Real-World Predictions

For temperature and salinity, we show the predictions and their corresponding uncertainty at multiple depths in Figure 5, and we compare the performance of our model to estimates from the FVCOM climatology. At the withheld test location (withheld from the surface extrapolation) between 2017 and 2022, we found that our model achieved a root-mean-square

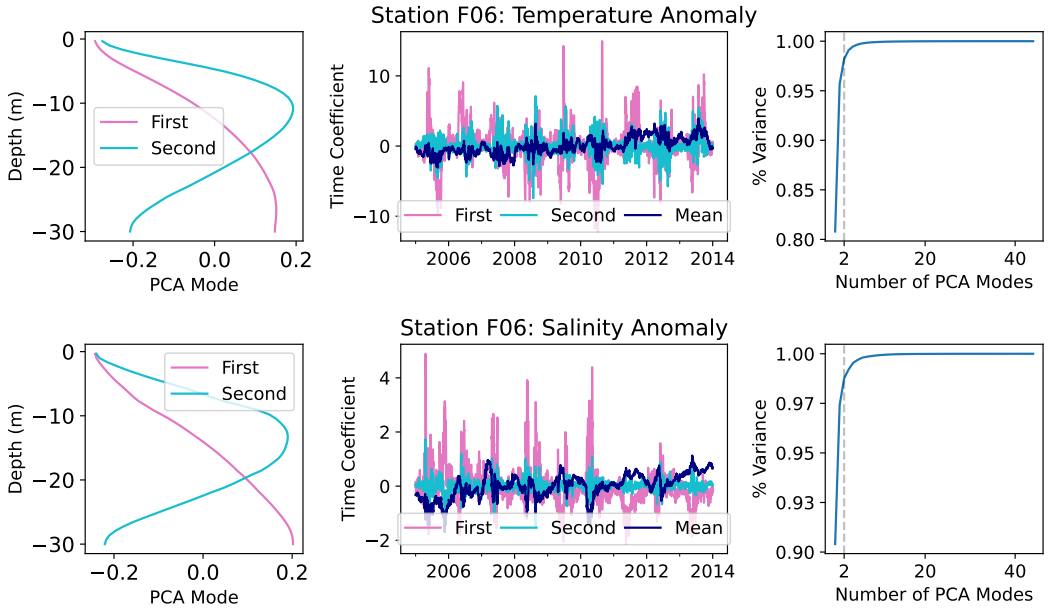

Figure 4: **Principal Component Analysis**. Results of PCA applied to temperature (top) and salinity (bottom) reanalysis of anomaly data at station F06. The PCA modes (left) show the shape of the in-depth modes. The PCA mean and coefficients (center) need to be predicted. The proportion of variance captured by each mode (right) confirms that two modes are sufficient to represent the data.

error (RMSE) of 1.54°C for temperature (compared to 1.78°C for climatology) and 0.35 for salinity (compared to 0.51 for climatology). These RMSE values for temperature and salinity are lower than the RMSE obtained from using the climatology, and our model is better for bias elimination.

5 Bayesian Regression: TA and DIC from Temperature, Salinity, and Surface Chlorophyll-a Concentration

In contrast to temperature and salinity, TA and DIC are non-conservative variables which are more difficult to predict with simplified numerical models because they are governed by complex transport, chemical, and biological processes. For these variables, we parameterized the hidden nonlinear correlations between conservative and non-conservative variables with standard regression methods. We use Bayesian regression models to estimate uncertainty. We train the regression models with a few hundred in-situ observations made at multiple dates, locations, and depths. Given the small number of observations for TA, DIC, and thus the estimated Ω_{Ar}, we only withheld observations from MWRA station F06 (42°10', -70°34'). For these variables, there is no existing 4D benchmark for the region of interest. We show the predictions from real-world observations at the withheld station F06 in addition to station F22 which is in the training set. Station F22 is the station with the most data points, and it is also the deepest.

For a given region of interest, there is a strong correlation between TA and salinity, so we used Bayesian ridge (linear) regression to predict TA from salinity (see Figure 6) [36, 37, 38]. The resulting regression coefficient and intercept were 57.04 and 349.43, respectively. These values were very close to the slope (54.6) and intercept (409) found in [23] for Buzzards Bay between 2015 and 2017. They were also in a similar range to the ones found from the model

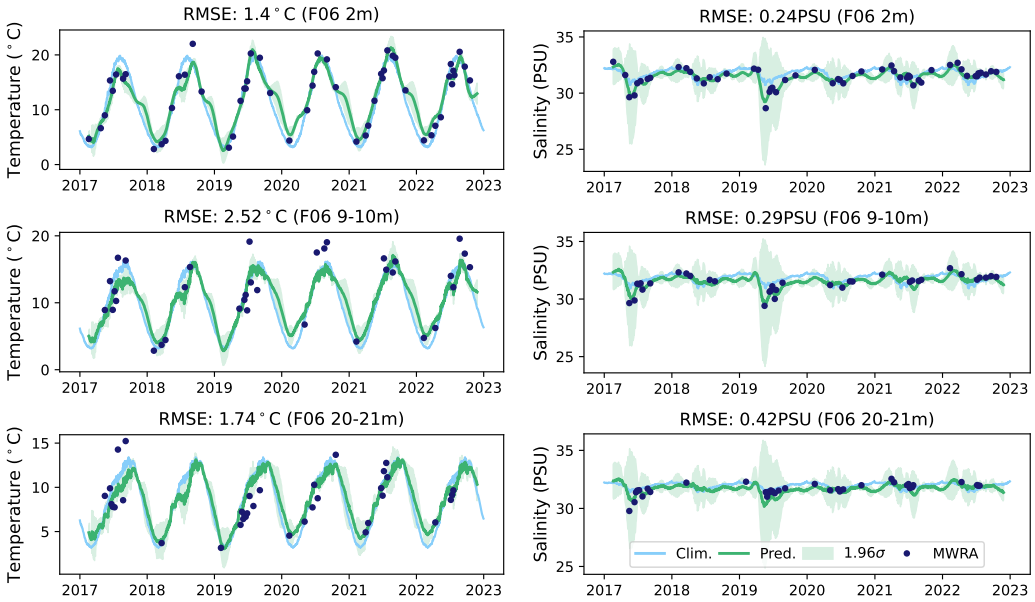

Figure 5: **Real-World Temperature and Salinity Predictions**. The blue line shows the climatology, the green line shows the predicted value (shading corresponds to one standard deviation), and the dark circles show the MWRA sensor measurements. Predicted values of temperature (left) and salinity (right) are for F06, a station withheld from surface extrapolations, at three depths in top, middle, and bottom panels.

in [38] for two data sets in George's Bank and Nantucket Shoals: slope of 52.5 and intercept of 497 in 2018 from the East Coast Ocean Acidification survey (ECOA-2) and slope of 55.9 and intercept of 371 for a historical data set. Our model achieved an overall training RMSE of 15.94 μmol·kg^{-1} and test RMSE of 12.29 μmol·kg^{-1} which are similar to the best test RMSE in the papers by McGarry (10.9 μmol·kg^{-1}) and Lima (9.0 μmol·kg^{-1}). These errors are also in the same range as those from a similar linear model for a larger region in [36] ($\sim 10\mu$mol·kg^{-1}). It is important to note that these relationships are only correct for the region of the ocean that is being studied, and new relationships need to be determined for other regions of interest [4].

For DIC, the relationship is not linear, so we use Gaussian process regression to model DIC as a function of temperature, salinity, and surface chlorophyll-a concentration. We build a new model for each "season" (April to June, July to September, and October to March), and each model is shown in Figure 7. A better model could have been obtained by using in-depth measurements for chlorophyll-a or oxygen, but we opted to use surface chlorophyll-a because it is readily available on a daily basis from satellites. As a result, we are able to make predictions for a larger spatial domain and at a higher temporal resolution. For this model, we remove outliers in the regressors using the Chauvenet criterion, but we keep all data points for DIC regardless of value. Our model achieved an overall train RMSE of 19.53 μmol·kg^{-1} and test RMSE of 33.83 μmol·kg^{-1} which are slightly higher than the best test RMSE in the papers by McGarry (11.2 μmol·kg^{-1}) and Lima (15.4 μmol·kg^{-1}). Our RMSE is highest for measurements between July and September which is consistent with other studies. The errors listed are computed using the in-situ observations from test locations as input as opposed to the predictions made by the neural network.

The final outputs computed with temperature and salinity inputs from the neural network predictions are shown for different depths in Figure 8 and 9. Even when using

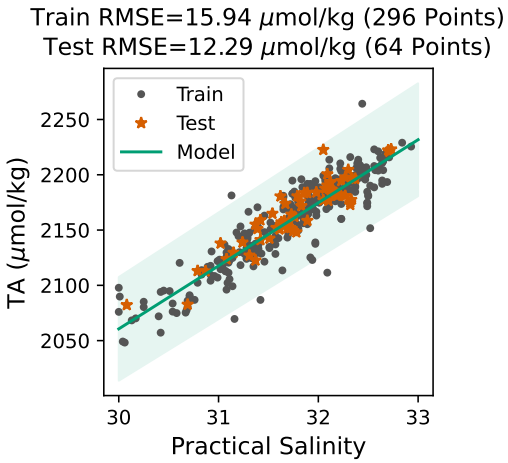

Figure 6: **TA Model**. Model produced by using Bayesian ridge regression to predict TA from salinity. The green shading corresponds to one standard deviation.

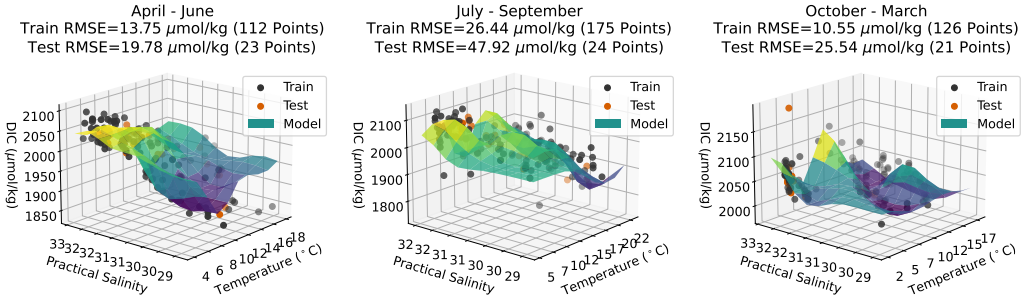

Figure 7: **DIC Model**. Models produced by using Gaussian process regression to predict DIC from temperature, salinity, and surface chlorophyll-a concentration for three seasons. The surfaces are generated for one set of values of chlorophyll-a concentration.

temperature and salinity from the neural network predictions, the RMSE remain within the same range. While the model can make predictions for many depths and seasons, we note that the RMSE is higher than the recommended value (10 μmol·kg^{-1}) for "weather" quality predictions — predictions that are useful for understanding short-term variations and spatial patterns at the scale of weather [19]. Errors were highest near the surface where there is more seasonal variability with significant drops in both TA and DIC. These observations can be explained by an increase in phytoplankton in the spring, followed by increased calcification and thermal stratification during the summer in the study area. Additional analysis is required to determine if any of the larger spikes can be explained by other events such as heavy rainfall. The DIC predictions are less smooth than the TA predictions due to the input from the chlorophyll — the satellite measurements for surface chlorophyll-a concentration exhibited high daily variability. The difference in the magnitude of the uncertainty between TA and DIC is due to the difference in the choice of the model (Bayesian regression as opposed to Gaussian process regression). However, only relative uncertainty is needed to make decisions about problems such as optimal sensor placement. Overall, the results suggest that more measurements are needed to produce high accuracy models, but the existing

model and uncertainty quantification can be used to make decisions about where and when to collect samples in the future.

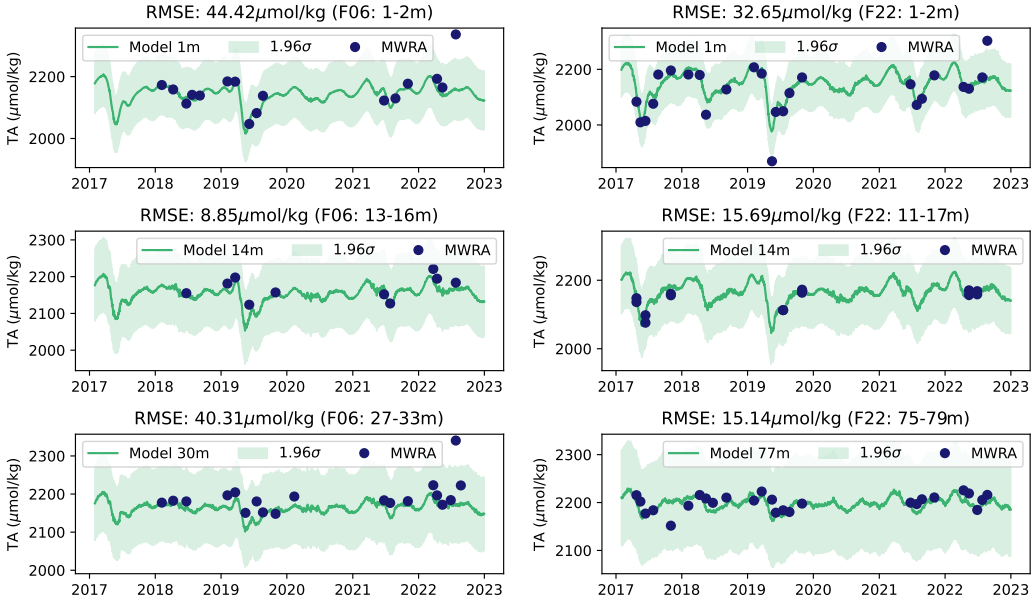

Figure 8: **Real-World TA Predictions**. Predicted TA at F06 and F22 for three depths obtained by passing predicted salinity into Bayesian ridge regression model. Here, the input salinity is obtained from the neural network predictions as opposed to real-world measurements.

6 Aragonite Saturation State from TA and DIC

We use the predicted TA and DIC to estimate Ω_{Ar} using the Python version of the marine carbonate system CO2SYS software, PyCO2SYS [39]. For the CO2SYS parameters, we set them in accordance with previous estimations made with the data set. We set the pH scale to the one from the National Bureau of Standards (NBS), the carbonic acid dissociation equilibrium constants to the ones from Lueker et al. 2000 [40], the bisulfate ion dissociation equilibrium constant to the one from Dickson et al. 1990 [41], the boron to salinity relationship to the one from Lee et al. 2010 [42], and the hydrogen fluoride dissociation equilibrium constant to the one from Dickson and Riley 1979 [43]. We note that we use the NBS scale for consistency, but it is less accurate than other options, especially when analyzing seawater. We compute the uncertainty of Ω_{Ar} by including the uncertainty for TA and DIC, found from the respective Bayesian regression models, as input parameters for the PyCO2SYS software.

We plot the distribution of errors in Figure 10, and we see that most points have an error near 0. We also observe that our model tends to underestimate Ω_{Ar} which is better than overestimation. Low values of Ω_{Ar} pose a greater risk to marine life and are therefore more important to detect. Final estimates of Ω_{Ar} at different depths are shown in Figure 11. These estimates are made using the TA and DIC predictions from Figures 8 and 9 which are in turn made with the predicted temperature and salinity from Figure 5.

As with TA and DIC, there is higher seasonal variability of Ω_{Ar} at the surface. Ω_{Ar} peaks during the spring and summer which is expected because of productivity from phytoplankton

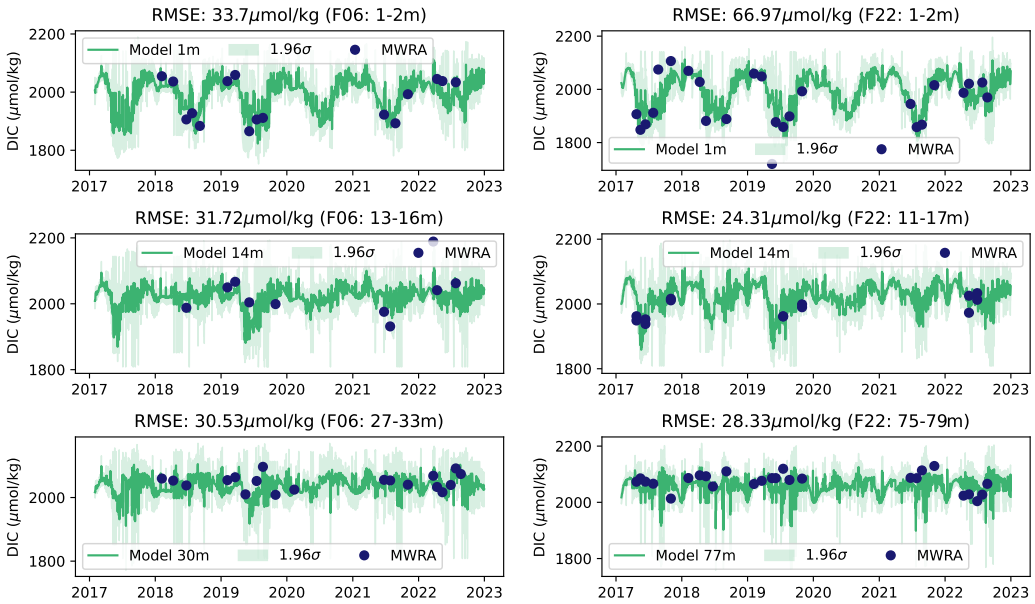

Figure 9: **Real-World DIC Predictions**. Predicted DIC (total CO_2) at F06 and F22 for three depths obtained by passing predicted temperature, salinity, and surface chlorophyll-a concentration into the Gaussian process regression model. Here, the input temperature and salinity are obtained from the neural network predictions, and the surface chlorophyll-a concentration is obtained from satellite data.

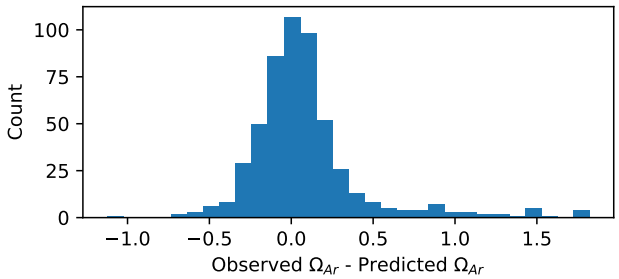

Figure 10: **Error of Ω_{Ar} Predictions**. Distribution of error of Ω_{Ar} predictions. Our model tends to slightly underestimate Ω_{Ar} which is of lower consequence than overestimation.

blooms and warmer water [44]. Given the importance of being able to determine drops in Ω_{Ar}, more measurements are needed during winter months and months with no data to fully assess the quality of the model. For example, the model predicted a significant drop in Ω_{Ar} between May and June of 2019, but the lack of measurements during that time period makes it difficult to validate this prediction.

7 Conclusion

We developed a machine learning framework to predict coastal seawater temperature, salinity, total alkalinity (TA), dissolved inorganic carbon (DIC), and carbonate saturation state (Ω_{Ar}) in 4D (latitude, longitude, depth and time), with reasonable accuracy and in real time using only surface measurements of temperature, salinity, and chlorophyll. The

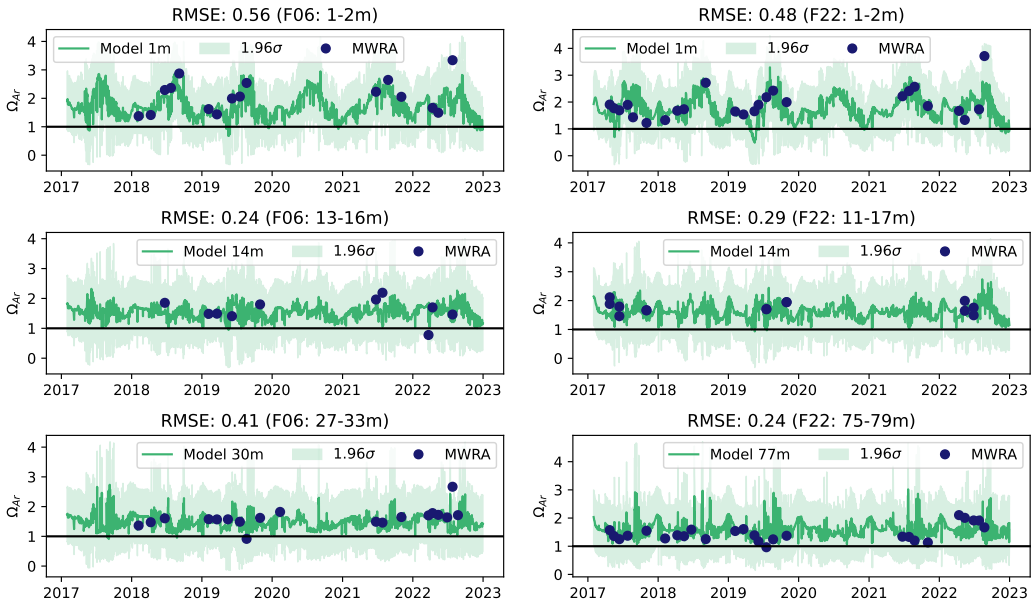

Figure 11: **Real-World Ω_{Ar} Predictions**. Predicted Ω_{Ar} at F06 and F22 for three depths obtained by passing predicted TA and DIC into CO2SYS software. Here, the input TA and DIC are obtained from the regression model predictions. The black line at $\Omega_{\mathrm{Ar}} = 1$ represents the threshold at which organisms with shells are most affected.

ability to model these properties given limited sensing capabilities is crucial to monitor the effects of climate change and the evolution of ocean and coastal acidification (OCA). We applied the framework to the Massachusetts Bay and Stellwagen Bank in the US Northeast Coast, and we found that the framework is superior in speed and resolution to other existing regional predictors. Furthermore, the framework provides an estimate for uncertainty which can be used for decision making related to many important tasks including ecosystem and resource management, identification of priority areas for mitigation, sensor selection, and optimal sampling.

8 Open Research

The temperature and chlorophyll satellite data are from Level 3 NASA Aqua-MODIS at https://oceancolor.gsfc.nasa.gov/l3/ [29]. The Massachusetts Water Resources Authority (MWRA) measurements were collected from a few different sources including MWRA, MIT Sea Grant, and Battelle, and the data were processed by the MWRA Environmental Quality Department (ENQUAL). More details can be found at https://www.mwra.com/our-environment/water-quality-reports and the full data set is available at https://github.com/becklabs/aragonite-opendap. The Finite Volume Community Ocean Model (FVCOM) used in the paper is produced for the Northeast Coastal Ocean Forecast System (NECOFS) from the Delaware Shelf to the eastern end of the Scotian Shelf. More details can be found at http://fvcom.smast.umassd.edu/necofs/. The temporal convolutional network was built with Tensorflow, the Gaussian process regression was implemented with GPy, and the Bayesian ridge regression was implemented with scikit-learn.

Acknowledgments
We want to acknowledge Justin Ries and Ryan Woosley for TA and DIC determinations.

MWRA provided in-situ data and continuous support in water sample collection during monthly surveys in Massachusetts Bay. In particular, we are very thankful to Betsy Reilley, David Wu, and Douglas Hersh from MWRA, and to Scott Libby, Alex Mansfield, and Matt Fitzpatrick from Battelle. This work was funded by MIT Sea Grant (NOAA Grant No. NA18OAR4170105) and the National Science Foundation Graduate Research Fellowship (Grant No. 2141064). Professor Chrys Chryssostomidis, former MIT Sea Grant director, pioneered the funding of research in ocean and coastal acidification. Ben Bray (MIT Sea Grant) has provided support in data visualization and prototypes towards an integrated web platform to calculate acidification parameters in the MA region. We also want to thank Ryan Woosley for stimulating discussions and Chen Changsheng for support in the use of FVCOM data.

References

[1] Josep G. Canadell, Corinne Le Quéré, Michael R. Raupach, Christopher B. Field, Erik T. Buitenhuis, Philippe Ciais, Thomas J. Conway, Nathan P. Gillett, R. A. Houghton, and Gregg Marland. Contributions to accelerating atmospheric CO2 growth from economic activity, carbon intensity, and efficiency of natural sinks. *Proceedings of the National Academy of Sciences*, 104(47):18866–18870, November 2007.

[2] Christopher L. Sabine, Richard A. Feely, Nicolas Gruber, Robert M. Key, Kitack Lee, John L. Bullister, Rik Wanninkhof, C. S. Wong, Douglas W. R. Wallace, Bronte Tilbrook, Frank J. Millero, Tsung-Hung Peng, Alexander Kozyr, Tsueno Ono, and Aida F. Rios. The Oceanic Sink for Anthropogenic CO2. *Science*, 305(5682):367–371, July 2004.

[3] M. Steinacher, F. Joos, T. L. Frölicher, G.-K. Plattner, and S. C. Doney. Imminent ocean acidification in the Arctic projected with the NCAR global coupled carbon cycle-climate model. *Biogeosciences*, 6(4):515–533, April 2009. ISSN 1726-4170.

[4] Taro Takahashi, Stewart C. Sutherland, David Chipman, John Goddard, Cheng Ho, Timothy Newberger, Colm Sweeney, and D. R. Munro. Climatological distributions of pH, pCO2, total CO2, alkalinity, and CaCO3 saturation in the global surface ocean, and temporal changes at selected locations. 164:95–125, 2014.

[5] James C. Orr, Victoria J. Fabry, Olivier Aumont, Laurent Bopp, Scott C. Doney, Richard A. Feely, Anand Gnanadesikan, Nicolas Gruber, Akio Ishida, Fortunat Joos, Robert M. Key, Keith Lindsay, Ernst Maier-Reimer, Richard Matear, Patrick Monfray, Anne Mouchet, Raymond G. Najjar, Gian-Kasper Plattner, Keith B. Rodgers, Christopher L. Sabine, Jorge L. Sarmiento, Reiner Schlitzer, Richard D. Slater, Ian J. Totterdell, Marie-France Weirig, Yasuhiro Yamanaka, and Andrew Yool. Anthropogenic ocean acidification over the twenty-first century and its impact on calcifying organisms. *Nature*, 437(7059):681–686, September 2005. ISSN 1476-4687.

[6] Dwight K. Gledhill, Meredith M. White, Joseph Salisbury, Helmuth Thomas, Ivy Mlsna, Matthew Liebman, Bill Mook, Jason Grear, Allison C. Candelmo, R. Christopher Chambers, Christopher J. Gobler, Christopher W. Hunt, Andrew L. King, Nichole N. Price, Sergio R. Signorini, Esperanza Stancioff, Cassie Stymiest, Richard A. Wahle, Jesica D. Waller, Nathan D. Rebuck, Zhaohui A. Wang, Todd L. Capson, J. Ruairidh Morrison, Sarah R. Cooley, and Scott C. Doney. Ocean and Coastal Acidification off New England and Nova Scotia. *Oceanography*, 28(2):182–197, 2015. ISSN 1042-8275.

[7] Rucheng Tian, Changsheng Chen, Jianhua Qi, Rubao Ji, Robert C. Beardsley, and Cabell Davis. Model study of nutrient and phytoplankton dynamics in the Gulf of Maine: patterns and drivers for seasonal and interannual variability. *ICES Journal of Marine Science*, 72(2):388–402, January 2015. ISSN 1095-9289, 1054-3139. doi: 10.1093/icesjms/fsu090. URL `https://academic.oup.com/icesjms/article/72/2/388/671414`.

[8] Justin B. Ries, Anne L. Cohen, and Daniel C. McCorkle. Marine calcifiers exhibit mixed responses to CO2-induced ocean acidification. *Geology*, 37(12):1131–1134, December 2009. ISSN 0091-7613. doi: 10.1130/G30210A.1. URL `https://doi.org/`

10.1130/G30210A.1. _eprint: https://pubs.geoscienceworld.org/gsa/geology/article-pdf/37/12/1131/3537229/i0091-7613-37-12-1131.pdf.

[9] Louise P. Cameron, Jonathan H. Grabowski, and Justin B. Ries. Effects of elevated pCO and temperature on the calcification rate, survival, extrapallial fluid chemistry, and respiration of the Atlantic Sea scallop Placopecten magellanicus. *Limnology and Oceanography*, 67(8):1670–1686, 2022. doi: https://doi.org/10.1002/lno.12153. URL https://aslopubs.onlinelibrary.wiley.com/doi/abs/10.1002/lno.12153. _eprint: https://aslopubs.onlinelibrary.wiley.com/doi/pdf/10.1002/lno.12153.

[10] Sa Siedlecki, J Salisbury, Dk Gledhill, C Bastidas, S Meseck, K McGarry, Cw Hunt, M Alexander, D Lavoie, Za Wang, J Scott, Dc Brady, I Mlsna, K Azetsu-Scott, Cm Liberti, Dc Melrose, Mm White, A Pershing, D Vandemark, Dw Townsend, C Chen, W Mook, and R Morrison. Projecting ocean acidification impacts for the Gulf of Maine to 2050. *Elementa: Science of the Anthropocene*, 9(1):00062, May 2021. ISSN 2325-1026. doi: 10.1525/elementa.2020.00062. URL https://online.ucpress.edu/elementa/article/9/1/00062/116976/Projecting-ocean-acidification-impacts-for-the.

[11] P Scott Libby, David G Borkman, W Rocky Geyer, Jeff T Turner, Amy S Costa, Christopher Goodwin, Jianjun Wang, and Dan L Codiga. 2021 Water Column Monitoring Results, December 2022.

[12] P Scott Libby, David G Borkman, W Rocky Geyer, Jeff T Turner, Amy S Costa, Christopher Goodwin, and Jianjun Wang. 2022 Water Column Monitoring Results. Technical report, Boston: Massachusetts Water Resources Authority., November 2023.

[13] Hannes Baumann and Erik M. Smith. Quantifying Metabolically Driven pH and Oxygen Fluctuations in US Nearshore Habitats at Diel to Interannual Time Scales. *Estuaries and Coasts*, 41(4):1102–1117, June 2018. ISSN 1559-2731. doi: 10.1007/s12237-017-0321-3. URL https://doi.org/10.1007/s12237-017-0321-3.

[14] Jason M. Hall-Spencer and Ben P. Harvey. Ocean acidification impacts on coastal ecosystem services due to habitat degradation. *Emerging Topics in Life Sciences*, 3(2):197–206, April 2019. ISSN 2397-8554. doi: 10.1042/ETLS20180117. URL https://doi.org/10.1042/ETLS20180117. _eprint: https://portlandpress.com/emergtoplifesci/article-pdf/3/2/197/851185/etls-2018-0117c.pdf.

[15] Rik Wanninkhof, Leticia Barbero, Robert Byrne, Wei-Jun Cai, Wei-Jen Huang, Jia-Zhong Zhang, Molly Baringer, and Chris Langdon. Ocean acidification along the Gulf Coast and East Coast of the USA. *Continental Shelf Research*, 98:54–71, 2015. ISSN 0278-4343. doi: https://doi.org/10.1016/j.csr.2015.02.008. URL https://www.sciencedirect.com/science/article/pii/S0278434315000473.

[16] Michelle D. Staudinger, Holly Goyert, Justin J. Suca, Kaycee Coleman, Linda Welch, Joel K. Llopiz, David Wiley, Irit Altman, Andew Applegate, Peter Auster, Hannes Baumann, Julia Beaty, Deirdre Boelke, Les Kaufman, Pam Loring, Jerry Moxley, Suzanne Paton, Kevin Powers, David Richardson, Jooke Robbins, Jeffrey Runge, Brian Smith, Caleb Spiegel, and Halley Steinmetz. The role of sand lances (Ammodytes sp.) in the Northwest Atlantic Ecosystem: A synthesis of current knowledge with implications for conservation and management. *Fish and Fisheries*, 21(3):522–556, 2020. doi: https://doi.org/10.1111/faf.12445. URL https://onlinelibrary.wiley.com/doi/abs/10.1111/faf.12445. _eprint: https://onlinelibrary.wiley.com/doi/pdf/10.1111/faf.12445.

[17] Ian R. Bricknell, Sean D. Birkel, Susan H. Brawley, Tyler Van Kirk, Heather J. Hamlin, Kyle Capistrant-Fossa, Kimberly Huguenard, G. Peter Van Walsum, Zhilong L. Liu, Longhuan H. Zhu, Gretchen Grebe, Emma Taccardi, Molly Miller, Brian M. Preziosi, Kevin Duffy, Carrie J. Byron, Charlotte T.C. Quigley, Timothy J. Bowden, Damian Brady, Brian F. Beal, Praveen K. Sappati, Teresa R. Johnson, and Shane Moeykens. Resilience of cold water aquaculture: a review of likely scenarios as climate changes in the Gulf of Maine. *Reviews in Aquaculture*, 13(1):460–503, 2021. doi: https://doi.org/10.1111/raq.12483. URL https://onlinelibrary.wiley.com/doi/abs/10.1111/raq.12483. _eprint: https://onlinelibrary.wiley.com/doi/pdf/10.1111/raq.12483.

[18] Eric J. Chapman, Carrie J. Byron, Rachel Lasley-Rasher, Christine Lipsky, Justin R. Stevens, and Rebecca Peters. Effects of climate change on coastal ecosystem food webs: Implications for aquaculture. *Marine Environmental Research*, 162:105103, 2020. ISSN 0141-1136. doi: https://doi.org/10.1016/j.marenvres.2020.105103. URL https://www.sciencedirect.com/science/article/pii/S0141113620305031.

[19] Ja Newton, Ra Feely, Eb Jewett, P. Williamson, J. Mathis, Eb Jewett, P. Williamson, and J. Mathis. Global Ocean Acidification Observing Network: Requirements and Governance Plan. December 2014. URL https://archimer.ifremer.fr/doc/00651/76343/.

[20] L. W. Juranek, R. A. Feely, W. T. Peterson, S. R. Alin, B. Hales, K. Lee, C. L. Sabine, and J. Peterson. A novel method for determination of aragonite saturation state on the continental shelf of central Oregon using multi-parameter relationships with hydrographic data. *Geophysical Research Letters*, 36(24):2009GL040778, December 2009. ISSN 0094-8276, 1944-8007. doi: 10.1029/2009GL040778. URL https://agupubs.onlinelibrary.wiley.com/doi/10.1029/2009GL040778.

[21] L. W. Juranek, R. A. Feely, D. Gilbert, H. Freeland, and L. A. Miller. Real-time estimation of pH and aragonite saturation state from Argo profiling floats: Prospects for an autonomous carbon observing strategy: ESTIMATING PH AND FROM ARGO FLOATS. *Geophysical Research Letters*, 38(17):n/a–n/a, September 2011. ISSN 00948276. doi: 10.1029/2011GL048580. URL http://doi.wiley.com/10.1029/2011GL048580.

[22] Catherine V. Davis, Kathryn Hewett, Tessa M. Hill, John L. Largier, Brian Gaylord, and Jaime Jahncke. Reconstructing Aragonite Saturation State Based on an Empirical Relationship for Northern California. *Estuaries and Coasts*, 41(7):2056–2069, November 2018. ISSN 1559-2723, 1559-2731. doi: 10.1007/s12237-018-0372-0. URL http://link.springer.com/10.1007/s12237-018-0372-0.

[23] Jennie E. Rheuban, Scott C. Doney, Daniel C. McCorkle, and Rachel W. Jakuba. Quantifying the Effects of Nutrient Enrichment and Freshwater Mixing on Coastal Ocean Acidification. *Journal of Geophysical Research: Oceans*, 124(12):9085–9100, December 2019. ISSN 2169-9275, 2169-9291. doi: 10.1029/2019JC015556. URL https://agupubs.onlinelibrary.wiley.com/doi/10.1029/2019JC015556.

[24] K. McGarry, S. A. Siedlecki, J. Salisbury, and S. R. Alin. Multiple Linear Regression Models for Reconstructing and Exploring Processes Controlling the Carbonate System of the Northeast US From Basic Hydrographic Data. *Journal of Geophysical Research: Oceans*, 126(2):e2020JC016480, February 2021. ISSN 2169-9275, 2169-9291. doi: 10.1029/2020JC016480. URL https://agupubs.onlinelibrary.wiley.com/doi/10.1029/2020JC016480.

[25] Ivan D. Lima, Zhaohui A. Wang, Louise P. Cameron, Jonathan H. Grabowski, and Jennie E. Rheuban. Predicting Carbonate Chemistry on the Northwest Atlantic Shelf Using Neural Networks. *Journal of Geophysical Research: Biogeosciences*, 128(7):e2023JG007536, July 2023. ISSN 2169-8953, 2169-8961. doi: 10.1029/2023JG007536. URL https://agupubs.onlinelibrary.wiley.com/doi/10.1029/2023JG007536.

[26] Lu Wang, Changsheng Chen, Joseph Salisbury, Robert Beardsley, and Jackie Motyka. Modeling of ocean acidification in the Massachusetts bay and Boston Harbor: 1-D experiments. 2024.

[27] Robert C. Beardsley Changsheng Chen, Hedong Liu. An Unstructured Grid, Finite-Volume, Three-Dimensional, Primitive Equations Ocean Model: application to Coastal Ocean and Estuaries. *Journal of Atmospheric and Oceanic Technology*, 20(1):159 – 186, 2003. Place: Boston MA, USA Publisher: American Meteorological Society Type: dataset.

[28] Bianca Champenois and Themistoklis P. Sapsis. Machine learning framework for the real-time reconstruction of regional 4D ocean temperature fields from historical reanalysis data and real-time satellite and buoy surface measurements. *Physica D: Nonlinear Phenomena*, 459:134026, 2024. ISSN 0167-2789. doi: https://doi.org/10.1016/j.physd.2023.134026. URL https://www.sciencedirect.com/science/article/pii/

S0167278923003809.

[29] NASA Ocean Biology Processing Group. Aqua MODIS Level 3 Mapped Chlorophyll Data, Version R2022.0, 2022. URL https://oceancolor.gsfc.nasa.gov/data/10.5067/AQUA/MODIS/L3M/CHL/2022.

[30] Andrew G. Dickson, Christopher L. Sabine, and James R. Christian. Guide to Best Practices for Ocean CO2 Measurements, 2007. URL https://www.ncei.noaa.gov/access/ocean-carbon-acidification-data-system/oceans/Handbook_2007.html.

[31] A. G. Dickson, J. D. Afghan, and G. C. Anderson. Reference materials for oceanic CO2 analysis: a method for the certification of total alkalinity. *Marine Chemistry*, 80(2):185–197, 2003. ISSN 0304-4203. doi: https://doi.org/10.1016/S0304-4203(02)00133-0. URL https://www.sciencedirect.com/science/article/pii/S0304420302001330.

[32] Carl Edward Rasmussen and Christopher K. I. Williams. *Gaussian Processes for Machine Learning*. Adaptive Computation and Machine Learning. Biologische Kybernetik, Cambridge, MA, USA, January 2006. Backup Publisher: Max-Planck-Gesellschaft.

[33] Hessam Babaee, C. Bastidas, Michael Defilippo, C. Chryssostomidis, and George Karniadakis. A Multi-Fidelity Framework and Uncertainty Quantification for Sea Surface Temperature in the Massachusetts and Cape Cod Bays. *Earth and Space Science*, 7, January 2020.

[34] Philip Holmes, John L. Lumley, and Gal Berkooz. Proper orthogonal decomposition. In *Turbulence, Coherent Structures, Dynamical Systems and Symmetry*, Cambridge Monographs on Mechanics, pages 86–128. Cambridge University Press, 1996.

[35] Zhong Yi Wan, Boyko Dodov, Christian Lessig, Henk Dijkstra, and Themistoklis P. Sapsis. A data-driven framework for the stochastic reconstruction of small-scale features with application to climate data sets. *Journal of Computational Physics*, 442:110484, October 2021.

[36] Wei-Jun Cai, Xinping Hu, Wei-Jen Huang, Li-Qing Jiang, Yongchen Wang, Tsung-Hung Peng, and Xin Zhang. Alkalinity distribution in the western North Atlantic Ocean margins. *Journal of Geophysical Research: Oceans*, 115(C8), 2010. doi: https://doi.org/10.1029/2009JC005482. URL https://agupubs.onlinelibrary.wiley.com/doi/abs/10.1029/2009JC005482. _eprint: https://agupubs.onlinelibrary.wiley.com/doi/pdf/10.1029/2009JC005482.

[37] Kitack Lee, Lan T. Tong, Frank J. Millero, Christopher L. Sabine, Andrew G. Dickson, Catherine Goyet, Geun-Ha Park, Rik Wanninkhof, Richard A. Feely, and Robert M. Key. Global relationships of total alkalinity with salinity and temperature in surface waters of the world's oceans. *Geophysical Research Letters*, 33(19), 2006. doi: https://doi.org/10.1029/2006GL027207. URL https://agupubs.onlinelibrary.wiley.com/doi/abs/10.1029/2006GL027207. _eprint: https://agupubs.onlinelibrary.wiley.com/doi/pdf/10.1029/2006GL027207.

[38] Christopher W. Hunt, Joseph E. Salisbury, Douglas Vandemark, Steffen Aßmann, Peer Fietzek, Christopher Melrose, Rik Wanninkhof, and Kumiko Azetsu-Scott. Variability of USA East Coast surface total alkalinity distributions revealed by automated instrument measurements. *Marine Chemistry*, 232:103960, 2021. ISSN 0304-4203. doi: https://doi.org/10.1016/j.marchem.2021.103960. URL https://www.sciencedirect.com/science/article/pii/S0304420321000451.

[39] Matthew P Humphreys, Abigail J Schiller, Daniel Sandborn, Luke Gregor, Denis Pierrot, Steven M A C van Heuven, Ernie R Lewis, and Douglas W R Wallace. PyCO2SYS: marine carbonate system calculations in Python, 2024.

[40] Timothy J Lueker, Andrew G Dickson, and Charles D Keeling. Ocean pCO2 calculated from dissolved inorganic carbon, alkalinity, and equations for $K1$ and $K2$: validation based on laboratory measurements of CO2 in gas and seawater at equilibrium. *Marine Chemistry*, 70(1):105–119, May 2000. ISSN 0304-4203. doi: 10.1016/S0304-4203(00)00022-0. URL https://www.sciencedirect.com/science/article/pii/S0304420300000220.

[41] Andrew G. Dickson. Standard potential of the reaction: AgCl(s) + 12H2(g) = Ag(s) + HCl(aq), and and the standard acidity constant of the ion HSO4 in synthetic sea water from 273.15 to 318.15 K. *The Journal of Chemical Thermodynamics*, 22(2): 113–127, 1990. ISSN 0021-9614. doi: https://doi.org/10.1016/0021-9614(90)90074-Z. URL https://www.sciencedirect.com/science/article/pii/002196149090074Z.

[42] Kitack Lee, Tae-Wook Kim, Robert H. Byrne, Frank J. Millero, Richard A. Feely, and Yong-Ming Liu. The universal ratio of boron to chlorinity for the North Pacific and North Atlantic oceans. *Geochimica et Cosmochimica Acta*, 74(6):1801–1811, 2010. ISSN 0016-7037. doi: https://doi.org/10.1016/j.gca.2009.12.027. URL https://www.sciencedirect.com/science/article/pii/S0016703709007789.

[43] A. G. Dickson and J. P. Riley. The estimation of acid dissociation constants in seawater media from potentiometric titrations with strong base. II. The dissociation of phosphoric acid. *Marine Chemistry*, 7(2):101–109, 1979. ISSN 0304-4203. doi: https://doi.org/10.1016/0304-4203(79)90002-1. URL https://www.sciencedirect.com/science/article/pii/0304420379900021.

[44] Zhaohui Aleck Wang, Gareth L. Lawson, Cynthia H. Pilskaln, and Amy E. Maas. Seasonal controls of aragonite saturation states in the Gulf of Maine. *Journal of Geophysical Research: Oceans*, 122(1):372–389, 2017. doi: https://doi.org/10.1002/2016JC012373. URL https://agupubs.onlinelibrary.wiley.com/doi/abs/10.1002/2016JC012373. _eprint: https://agupubs.onlinelibrary.wiley.com/doi/pdf/10.1002/2016JC012373.